SPE 7114

Gas Injection for Upstructure Oil Drainage

R. F. Strickland, SPE-AIME, Texas A&M U.
R. A. Morse, SPE-AIME, Texas A&M U.

Introduction

Oil recovery from high-relief reservoirs can be increased by downstructure gas injection. In this process, often called "attic oil recovery," gas is injected in the structurally highest well in the reservoir. The injected gas will migrate upstructure, forming a secondary gas cap and displacing oil downward.

In high-relief reservoirs, which typically occur around "piercement type" salt domes, field development is complicated by the lack of control on the upper limits of the structure. To ensure a commercial completion, operators usually locate development wells a safe distance from the estimated sand/salt interface. In reservoirs with an active bottomwater drive, much of the updip oil will not have been produced when the highest well in the structure waters out. Sidetracking or drilling new wells is expensive and risky. It would be almost impossible to locate new wells to drain all updip oil adequately. Reservoirs with steep dip and high permeability allow injected gas to migrate to the most inaccessible areas of the pinchout, providing good lateral coverage. Injected gas may be traded economically for oil as long as the price of a unit volume of reservoir oil is sufficiently greater than the price of a corresponding unit volume of reservoir gas.

Many authors[1-5] have reported on field applications of the attic oil recovery process. In 1971, Combs and Knezek[6] published theoretical guidelines and field data concerning the maximum gas/oil segregation rate and the minimum and actual gas requirements to recover 1 bbl oil.

This paper presents results of a numerical model study of an attic oil recovery process and defines the variables that control the reservoir performance of a successful project. A method is presented to calculate the required gas injection volumes.

Numerical Model

The numerical model used in this study is a conventional beta model that was modified to simulate the attic oil recovery process properly. The model includes these features: three-phase flow of oil, water, and gas; gas/oil solubility; gas/oil and oil/water capillary pressure; three-phase relative permeability[7] with hysteresis effects[8]; variable bubble-point scheme[9]; variable flow rates; gravity effects, both areally and vertically; conformance to any reservoir geometry; and variable rock and fluid properties.

Even with the advent of relatively efficient three-dimensional reservoir simulators, computing costs for a meaningful study can become expensive. A two-dimensional areal model can simulate the same problem, provided the distribution and flow of fluids in the vertical dimension is included implicitly in the areal model. Several authors[10-13] have reported on the theory and calculation techniques of "pseudofunctions." Jacks *et al.*[10] presented a technique for calculating the "dynamic pseudofunctions" that could be applied over a wide range of flow rates and initial fluid saturations. Our

0149-2136/79/0010-7114$00.25

Any attic oil project tries to displace with gas the oil located above the structurally highest well in the reservoir. Results from a numerical simulator show that the most important controllable variable in attic oil recovery is the volume of gas injected during each cycle. A method is presented for calculating the required gas injection volume for each cycle of an attic oil project.

numerical model incorporates a technique similar to that described by Jacks *et al.* A complete description and validation of the numerical model was presented by Strickland and Morse.[14]

Description of Recovery Process

In a single-well reservoir, the same well is used for both injecting gas and producing oil. The steps in an attic oil recovery process are (1) the well is produced until it waters out, (2) gas is injected, (3) the well is shut in to allow the gas to migrate upstructure, and (4) the well is put back on production. This process is repeated until all upstructure oil has been produced. If too much gas is injected, oil may be displaced below the level of the original oil/water contact. Originally, no residual oil saturation existed below this level. If any oil moves into this zone, a portion can be trapped as residual saturation and will be lost when production resumes.

As gas is injected into a tilted reservoir, it migrates upstructure because it is lighter than oil. As theorized by Combs and Knezek,[6] Fig. 1 shows the location of the injected gas for injection rates above and below the "maximum segregation rate." They theorized that the gas should be prevented from moving downdip by maintaining the injection rates at less than or equal to the maximum segregation rate. Even if the gas has moved downdip during the injection period, most of the gas will migrate upstructure when the well is shut in. However, some gas will be trapped because of relative permeability hysteresis. When the well is put back on production, water will begin to move upstructure. The injected gas, like the downward moving oil, should not be allowed to migrate below the level of the original oil/water contact.

Reservoir Description

The physical situation simulated was a 2,000-ft.-long reservoir with a dip angle of 27°. The basic reservoir and fluid properties are described in Table 1. The only producing well was located in the center of the reservoir. Because the system was symmetrical, only half the reservoir had to be simulated. The relative permeability and capillary pressure curves are shown in Figs. 2 through 4. Pressure dependent properties are presented in Table 2.

To determine the effect of grid size, one cycle of attic oil production was simulated with several different grid patterns. The final grid pattern for all simulations is shown in Fig. 5. In the vertical section there is a fine grid breakup at the top of the formation to simulate the upstructure migration of gas properly. The areal grid pattern uses a fine breakup around the well to study the areal movement and distribution of the injected gas.

A strong bottomwater drive was simulated by assigning a very large porosity to one cell in the water zone. The single-well reservoir was produced at a constant rate of 400 STB/D fluid until a WOR of 3.0 was reached. At this time, after 7.58 years of production, 37% of the original oil in place (699,650 STB) has been produced. As fluid was produced, the reservoir pressure was lowered slightly, causing gas to come out of solution and migrate to the top of the structure, forming a secondary gas cap. A 10% gas saturation and a 60% water saturation profile are shown in Fig. 6.

TABLE 1—RESERVOIR PROPERTIES

Reservoir length, ft	2,000
Reservoir thickness, ft	50
Reservoir width, ft	1,000
Dip angle, degrees	27
Porosity, %	20
Permeability, md	500
Pressure datum, ft subsea	−3,000
Original pressure, psi at datum	1,100
Bubble-point pressure, psia	2,400
Oil/water contact, ft subsea	−3,800
Oil density, psi/ft	0.392
Water density, psi/ft	0.5
Oil formation volume factor, RB/STB	1.2679
Water formation volume factor, RB/STB	1.0
Oil viscosity, cp	1.0
Water viscosity, cp	1.01
Gas viscosity, cp	0.01

TABLE 2—PRESSURE-DEPENDENT FLUID PROPERTIES

Pressure (psia)	Solution Gas (Mscf/STB)	Gas Density (psi/ft)	B_g (RB/Mscf)
2,000	0.6307	0.0784	0.8551
1,600	0.5213	0.0640	1.0198
1,200	0.4119	0.0467	1.3988
800	0.3026	0.0287	2.2671
500	0.2179	0.0165	3.9573
400	0.1864	0.0127	5.1361
300	0.1548	0.0091	7.148
200	0.1157	0.0058	11.364
100	0.0667	0.0027	24.45

Combs and Knezek Theory

Combs and Knezek presented a method to calculate the maximum gas/oil segregation rate. They theorized that the gas injection rate should not exceed the maximum gas/oil segregation rate to prevent gas from moving downdip. The maximum segregation rate was related to the physical parameters of the reservoir, the mobility ratio, the density difference of the fluids, and the fraction

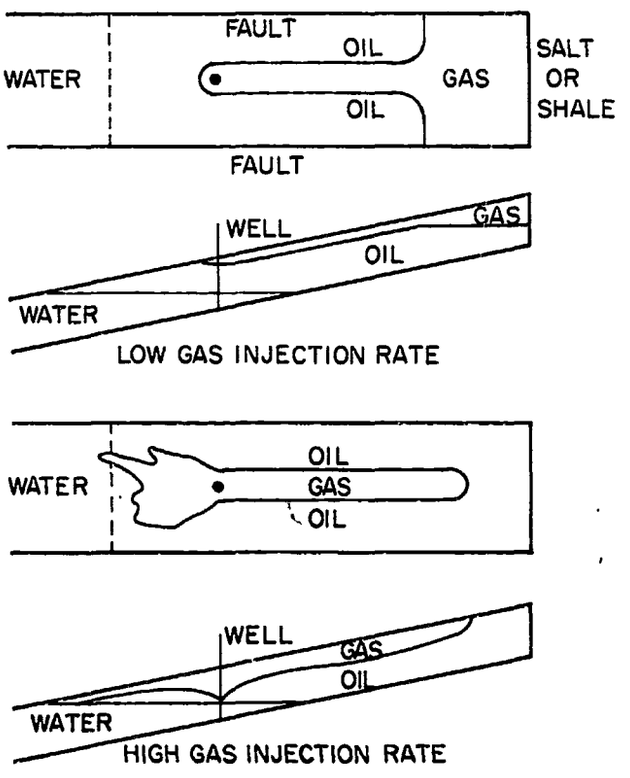

Fig. 1—Location of injected gas (low and high rates).

of the area occupied by the gas finger.

When developing the equation for the maximum segregation rate, they assumed the following criteria.

1. The reservoir pressure is held constant by a strong water drive.
2. The gas moves upward in a "finger" that has the maximum possible gas saturation.
3. The rest of the fault block contains no gas saturation, and the oil flows downward through this region.
4. The flow rate of oil downdip must equal the flow rate of gas updip.

Combs and Knezek also stated that the most important controllable variable in the operation of single-well projects is the rate of gas injection relative to the maximum segregation rate. They theorized that as the

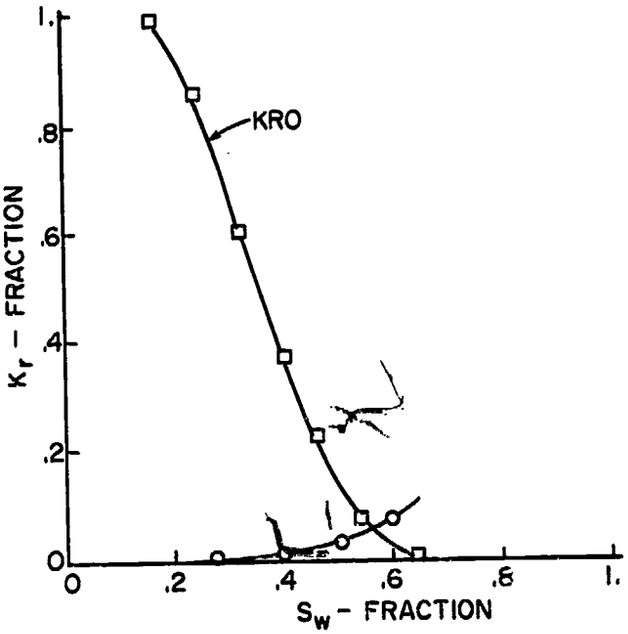

Fig. 2—Oil/water relative permeability.

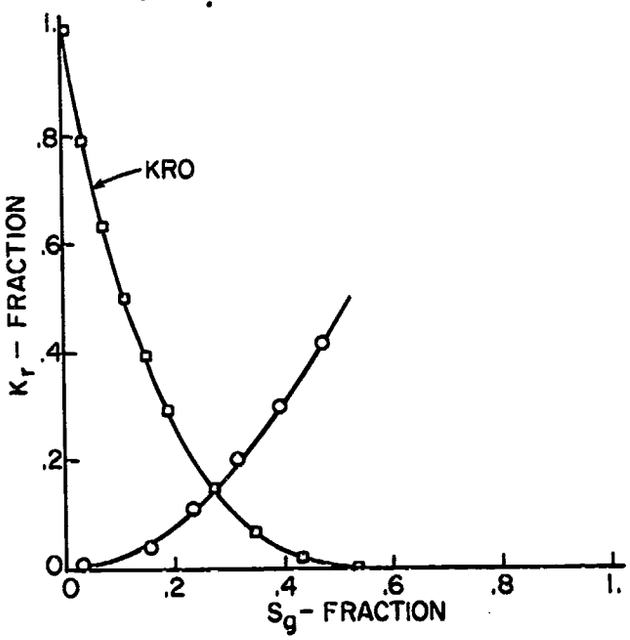

Fig. 3—Gas/oil relative permeability.

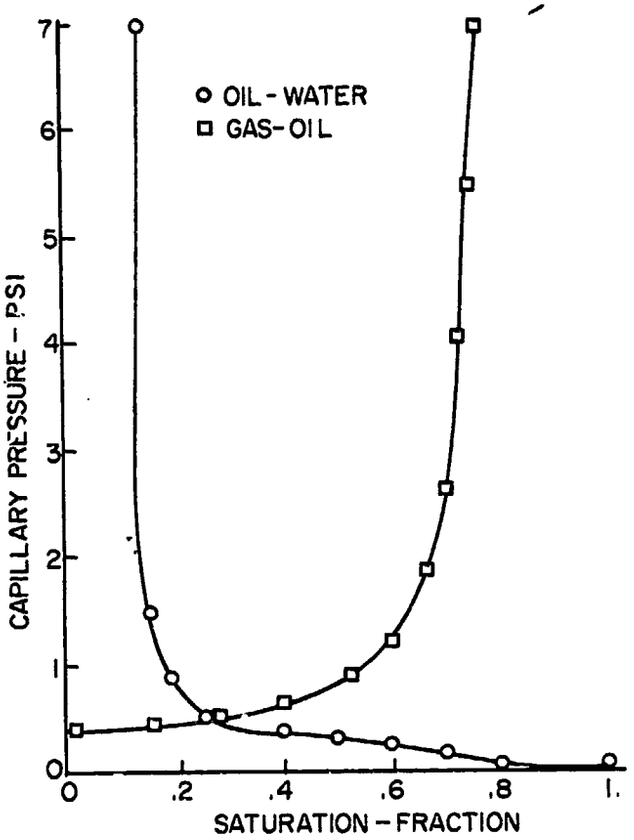

Fig. 4—Capillary pressure.

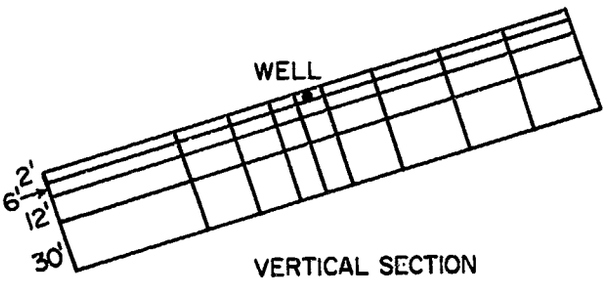

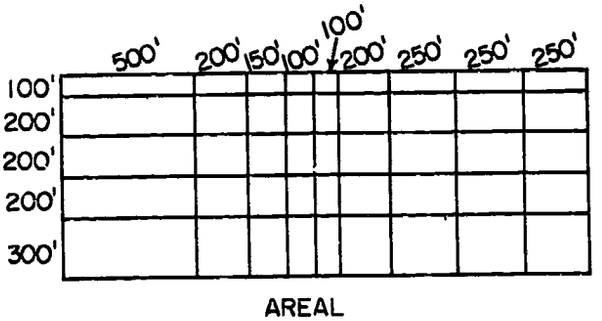

Fig. 5—Grid pattern of a well.

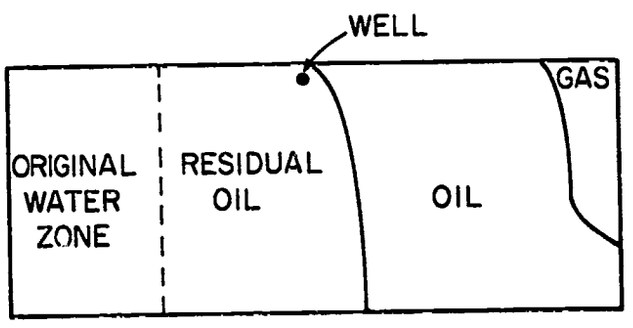

Fig. 6—Positions of oil/water and gas/oil contacts.

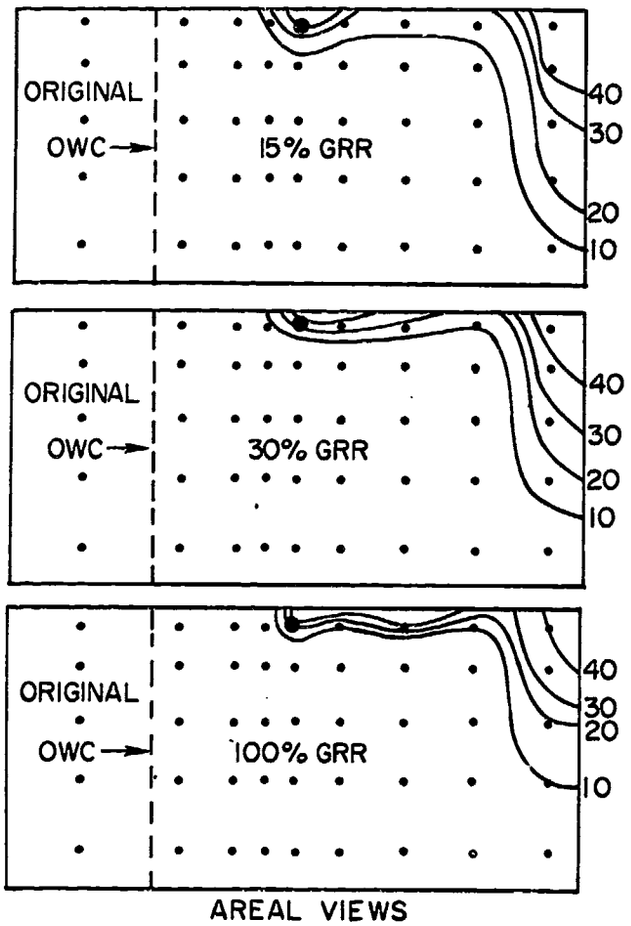

Fig. 7—Gas saturation contours at 100 MMscf gas injected.

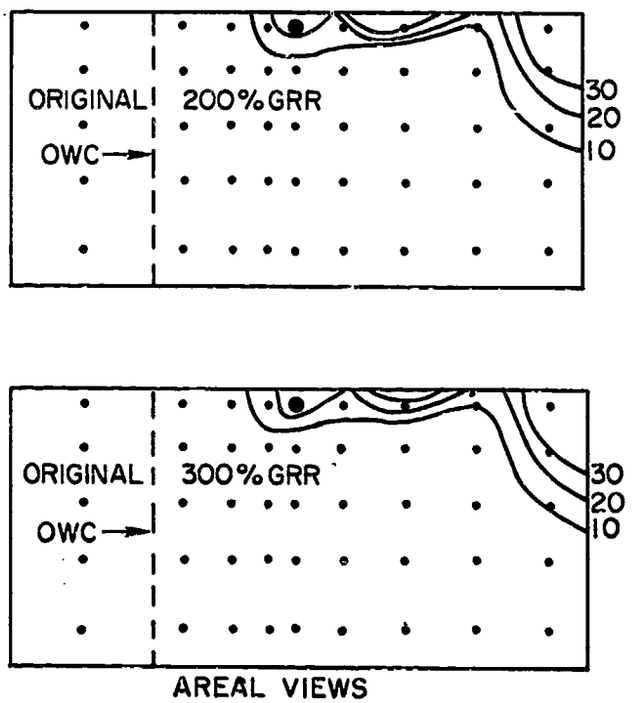

Fig. 8—Gas saturation contours at 100 MMscf gas injected.

gas injection rate approached the maximum segregation rate, the size of the gas finger would increase rapidly. For the reservoir described, the maximum segregation rate was calculated as 2,519 STB/D, which is equivalent to a gas injection rate of 2,309 Mscf/D at a pressure of 1,205 psia — the reservoir pressure at the producing well at the end of the production cycle.

Here, all gas injection rates are referred to as a percent of the "gravity reference rate" (GRR), which has been described fully by Terwilliger *et al.*[15] This reference rate is defined by the following equation.

$$GRR = 1.127 \frac{K_L}{\mu_L} g \Delta \rho \sin \alpha .$$

For this system, the GRR is 3,891 RB/D, which is equivalent to a gas injection rate of 2,796 Mscf/D at a pressure of 1,205 psia. The maximum segregation rate of Combs and Knezek[6] is 82.6% of the GRR.

Effect of Gas Injection Rate

Several simulations were conducted to determine the effect of the gas injection rate. Fig. 7 shows an areal view of the reservoir with gas injection profiles after 100 MMscf gas had been injected at rates of 15, 30, and 100% of the GRR, respectively. The size of the gas finger extending upward into the gas cap was approximately the same for all three injection rates. For the injection rate of 100% of the GRR, the areal coverage of the free gas was much less than the coverage at an injection rate of 15% of the GRR. As the injection rate increased, reservoir pressure also increased. Because the same volume of gas was injected in each case, higher pressures resulted in less areal coverage. Combs and Knezek also suggested that if the gas injection rate was greater than the maximum segregation rate, all gas in excess of the maximum segregation rate would move downdip. Fig. 8 shows the areal gas injection profiles after 100 MMscf gas had been injected at rates of 200 and 300% of the GRR. These rates correspond to 242 and 363% of the maximum segregation rate, respectively.

At the end of the first production period, the reservoir pressure was lower than the original pressure. A secondary gas cap had formed and a small amount of free gas (1 to 2%) existed throughout the reservoir below the gas cap. As gas was injected and reservoir pressure increased, the gas saturation decreased, resulting in the trapping of the free gas because of relative permeability hysteresis. In some areas of the reservoir, the pressure increased enough to force all trapped gas back into solution. However, near the well the injected gas flowed radially outward, contacted the trapped gas, increased the saturation, and allowed flow before all the trapped gas went back into solution. In every case (from 15 to 300% of the GRR), the injected gas flows radially away from the well until gravity forces dominate and the gas migrates upward into the gas cap. Only a small increase in gas saturation was required for the trapped gas to begin flowing. Therefore, the injected gas easily formed a continuous finger into the gas cap. The injected gas did not move upward in a finger having the maximum possible gas saturation as proposed by Combs and Knezek. A substantial amount of gas/oil counterflow did exist in the gas finger. However, in most areas of the reservoir, the pressure increased enough to force all

TABLE 3—PRESSURE AND SATURATION DISTRIBUTIONS AFTER 100 MMscf INJECTED GAS

Injection Rate (% GRR)	Location: Water Zone Pressure (psi)	Water Zone S_o (fraction)	Water Zone S_g (fraction)	Well: Injection Pressure (psi)	Well S_o (fraction)	Well S_g (fraction)	Gas Cap Pressure (psi)	Gas Cap S_o (fraction)	Gas Cap S_g (fraction)
Initial	1,461	0.0	0.0	1,304	0.90	0	1,132	0.92	0
15	1,463	0.0	0.0	1,370	0.34	0.31	1,239	0.44	0.48
30	1,464	0.0	0.0	1,416	0.33	0.28	1,299	0.48	0.43
60	1,465	0.0	0.0	1,472	0.30	0.36	1,336	0.48	0.43
100	1,466	0.0	0.0	1,484	0.31	0.31	1,357	0.51	0.41
200	1,477	0.0	0.0	1,508	0.32	0.28	1,359	0.56	0.36
300	1,478	0.0	0.0	1,542	0.32	0.29	1,362	0.59	0.33

trapped gas back into solution. Most downward migration of oil occurred through this region of no gas saturation.

As high-pressure gas was injected into the well, it migrated upstructure to the lower-pressure region of the original gas cap. When the injected gas moved away from the well, it had to displace oil. The displaced oil could compress the original gas cap easier than it could push water back into the water zone. Therefore, even at very high injection rates, the gas will move preferentially upward into the gas cap. In the lower-pressure gas cap, the gas could expand by a factor of 1.3, resulting in a more economical displacement of oil with gas. Figs. 7 and 8 show that as the injection rate increased from 15 to 300% of the GRR, the areal coverage decreased. The effect of injection rate on oil recovery will be shown in a later section. Table 3 summarizes the pressure and saturation distributions at injection rates ranging from 15 to 300% of the GRR.

Effect of Gas Injection Volume

At the end of the first production cycle, 699,650 STB oil has been produced. To replace the reservoir voidage would require that 573.7 MMscf gas be injected at the original reservoir pressure. However, the maximum volume of gas that could be injected would equal the reservoir volume of water that could be moved from the watered-out zone back into the water zone. Above the water/oil transition zone, the initial water saturations ranged from 8 to 12%. As fluid was produced and the water/oil contact advanced to the level of the well, the water saturation reached a maximum of 64%. This also corresponds to the average saturation behind a front calculated from Buckley-Leverett theory. The injected gas migrated upstructure, displaced oil, and caused a downward-moving displacement of water by oil. During the oil/water drainage process, the minimum attainable water saturation was a function of the gas injection rate. As the gas injection rate increased the average water saturation behind the oil-water front also increased. Fig. 9 shows the fractional flow curves for the displacement of water by oil at three different gas injection rates. At a very low gas injection rate (28 Mscf/D), the average water saturation behind the front was 27%, while at a high gas injection rate (8,388 Mscf/D), the average water saturation was 47%. The three gas injection rates and the average water saturations also are compared with the oil/water GRR in Table 4. For example, a gas injection rate of 28 Mscf/D is equivalent to 46.4 RB/D. This also equals 1.2% of the gas/oil GRR of 3,891 RB/D. From the simulation run the pore volume and the water saturation in each grid block at the end of the production cycle were known. The total movable water during the oil/water drainage process was calculated to be either 463,500 res bbl with a 27% irreducible water saturation, or 196,000 res bbl with a 47% irreducible water saturation. The maximum gas injection volumes

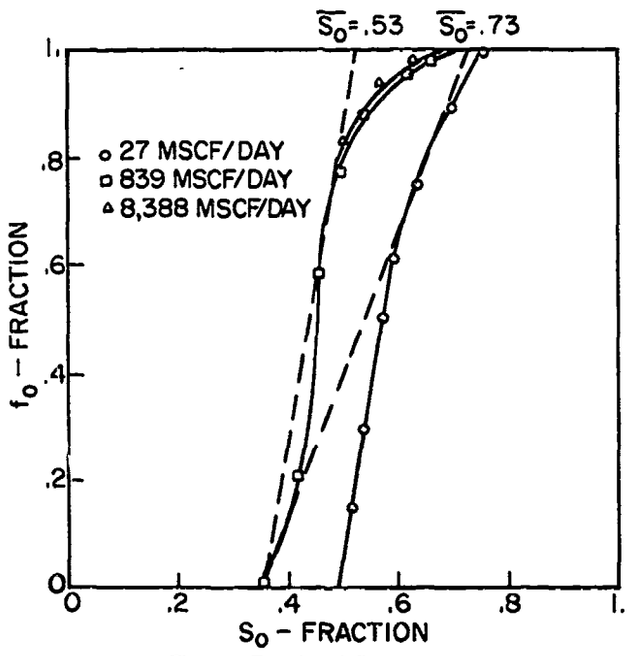

Fig. 9—Fractional flow curves.

TABLE 4—COMPARISON OF GRR WITH AVERAGE WATER SATURATIONS

	Gas Injection Rate (Mscf/D) 28.0	838.8	8,388.0
Average reservoir pressure during gas injection, psia	1,037	1,141	1,193
Gas formation volume factor, RB/Mscf	1.66	1.56	1.41
Injection rate, RB/D	46.4	1,310.	11,810.
Injection rate, % gas/oil GRR	1.2	34	303
Injection rate, % oil/water GRR	3.8	108	970
Average S_o behind front, fraction (Fig. 9)	0.73	0.53	0.53
Average S_w behind front, fraction	0.27	0.47	0.47

Gas/oil GRR = 3,891 RB/D.
Oil/water GRR = 1,218 RB/D.

TABLE 5—MAXIMUM GAS INJECTION VOLUMES WITHOUT DISPLACING OIL INTO THE WATER ZONE

Total Movable Water Calculated from Simulation (res bbl)	Injection Rate (Mscf/D)	B_g (RB/Mscf)	Maximum Injected Volume (MMscf)
463,500	28	1.66	279.5
196,100	838.8	1.56	125.3
196,100	8,388	1.41	139.3

are shown in Table 5.

Fig. 10 shows an areal view of a 5% gas saturation contour, indicating the extent of the injected gas after 160 MMscf gas had been injected at rates indicated in Tables 4 and 5. At the lowest rate, all gas was migrating into the gas cap, while no oil migrated below the level of the original oil/water contact. With an injection rate of 838.8 Mscf/D, the expanding gas pushed the oil below the level of the original oil/water contact. At the highest injection rate, both oil and gas had moved into the original water zone.

To prevent the movement of oil or gas into the water zone during a cycle of an attic oil recovery project, the cumulative gas injected should not exceed the total movable water. From a simulation run the total movable water easily is calculated from the irreducible water saturation during the oil flood, the pore volume, and water saturations in each grid block at the end of the production cycle. From field data a good approximation of the total movable water can be calculated by knowing the fractional flow curves and cumulative oil production. The average water saturation in the flooded-out portion of the reservoir can be obtained from the f_w vs S_w curve. The average oil saturation, after the flooded-out portion of the reservoir has been resaturated with oil at the end of the gas injection cycle, can be obtained from the f_o vs S_o curve. The total flow rate used in the f_o calculation is the gas injection rate expressed in reservoir barrels per day.

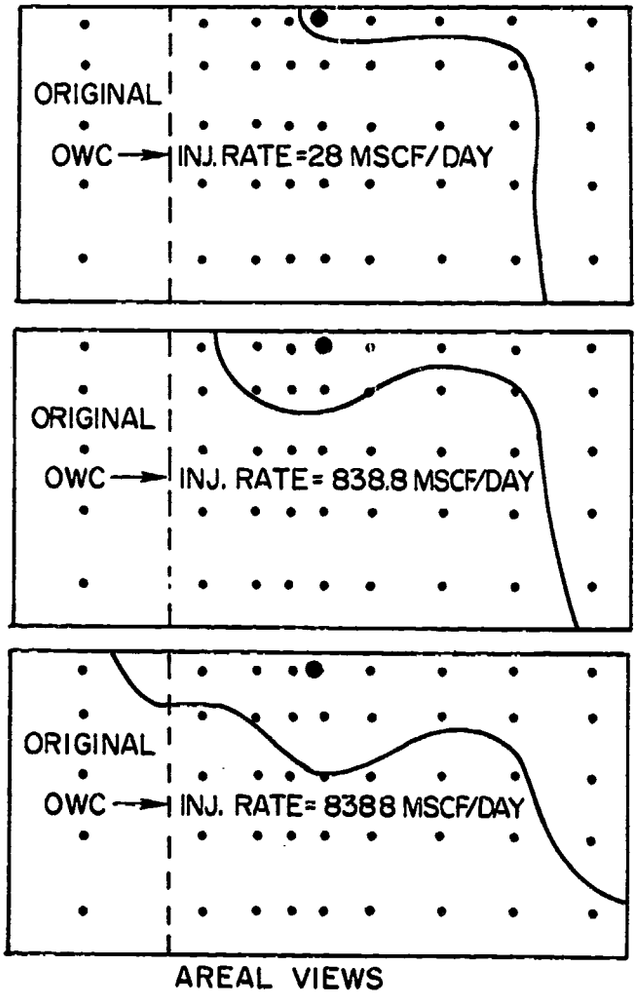

Fig. 10—5% gas saturation contour at 16 MMscf gas injected.

The cumulative oil production, converted to reservoir barrels, equals the water influx, assuming all produced oil was displaced with water. The effective pore volume of the flooded-out region equals the water influx divided by the difference between the average water saturation, from f_w vs S_w, and the initial water saturation. At the end of the oil flood, the movable water equals the effective pore volume times the difference between the average water saturation before the oil flood and the residual water saturation after the oil flood. The residual water saturation equals $1 - \bar{S}_o$, where $\bar{S}_o$ is from an f_o vs S_o graph. For comparison, three simulations of a strong bottomwater drive reservoir were made with the following initial conditions: (1) Run 1 — no solution gas (dead oil), (2) Run 2 — with solution gas starting at the bubble point (gas came out of solution and formed a secondary gas cap during the production cycle), and (3) Run 3 — with solution gas starting 1,000 psia above the bubble point. In each case, the true movable water was calculated from the saturation distribution at the end of the production period. In Run 3, the initial oil/water contact was at a higher level than in Runs 1 or 2, resulting in less oil production before a WOR of one was reached. Table 6 compares the actual with calculated movable water for the three runs. In Runs 1 and 3, the percent error is negative, while a positive percent error occurred in Run 2. The expanding gas cap created during the production cycle tended to maintain higher oil rates. In this case, all produced oil was not displaced with water. If little solution gas exists or if the reservoir is producing oil above the bubble point, then this calculation procedure yields a conservative estimate of the movable water and, therefore, the required gas injection volume. If a secondary gas cap has formed, the calculated movable water will be too high.

Reservoir Performance Comparison

Several simulations were made to compare the performance of successive cycles of an attic oil project. In Table 7, the performance of two and three cycles of a single-well project are shown at injection rates of 30 to 300% of the GRR. In all cases, approximately 90 MMscf gas was injected per cycle. The average rates were obtained by dividing the oil produced for each cycle by the cycle length. The ratio of the oil produced to

TABLE 6—MOVABLE WATER CALCULATIONS

Item	Run 1	Run 2	Run 3
WOR at end of production cycle	1.09	1.09	1.08
Cumulative oil production, STB	525,165	503,560	333,190
Cumulative oil production, res bbl	665,800	638,400	422,400
Water influx, res bbl	665,800	638,400	422,400
Initial water saturation	0.112	0.114	0.143
Effective pore volume, res bbl $PV = \frac{N_p B_o}{(S_w - S_{wi})}$	1,261,000	1,214,000	850,000
Calculated movable water, res bbl PV $(S_w - S_{wi})$	214,360	206,300	144,500
True movable water (from simulation), res bbl	220,200	200,600	156,000
Percent error, %	−2.65	2.8	−7.4

$\bar{S}_w$ from f_w vs S_w = 0.64.
$\bar{S}_o$ from f_o vs S_o (Fig. 9) = 0.53.
$S_{wr} = 1 - \bar{S}_o = 0.47$.

the volume of gas injected gives an indication of the effectiveness of oil displaced by gas.

In all cases, the oil produced per cycle, the water produced per cycle, and the cycle length decreased with each successive cycle. During the first cycle, the size of the gas cap was increased by gas coming out of solution as the pressure decreased. In each following cycle, less existing oil contributed solution gas to the expansion of the gas cap. The cumulative oil produced at the end of each cycle was independent of the injection rate.

Effect of Bubble-Point Pressure

Several simulations were made of a bottomwater drive reservoir producing oil at a pressure above the original bubble point to determine the effect of gas injection rate and gas injection volume under these conditions. The bubble-point pressure was 1,000 psia, and the original reservoir pressure was 2,000 psia. At the end of the production cycle (WOR = 3.0), the reservoir was still 950 psia above the bubble point. From Table 6 (Run 3) the movable water calculated from the simulation was 150,286 res bbl, which is equivalent to 175 MMscf gas injected at the original reservoir pressure. This movable water was calculated at the high rates of injection (839 to 8,388 Mscf/D), which yielded an irreducible water saturation of 0.47. If gas is injected at a low rate (28 Mscf/D), the total movable water would be 346,386 res bbl or 405 MMscf gas at 2,000 psia.

Gas was injected at three different rates — 27, 839, and 2,796 Mscf/D — for a cumulative injection of 400 MMscf. Fig. 11 shows an areal view of the gas saturation profiles for the injection rates of 27 and 839 Mscf/D after 400 MMscf had been injected. Initially, all injected gas went into solution until the bubble point of the oil was raised to the level of the reservoir pressure and free gas could then exist. In both cases, all injected gas that did not go into solution migrated uniformly to the top of the formation. At the low rate of injection, the oil/water level was still 150 ft above the original contact. This indicates that not enough gas was injected to displace the oil down to the level of the original oil/water contact. Some injected gas was lost as it went into solution in the undersaturated oil. However, at an injection rate of 839 Mscf/D, a substantial volume oil (85,330 STB) had been displaced below the level of the original oil/water contact. An injection rate of 839 Mscf/D yields a 47% irreducible water saturation during the waterflood, which results in a lower maximum gas

TABLE 7—RESERVOIR PERFORMANCE COMPARISON

	Injection Rate										
	30% GRR		100% GRR			200% GRR			300% GRR		
	1st Cycle	2nd Cycle	1st Cycle	2nd Cycle	3rd Cycle	1st Cycle	2nd Cycle	3rd Cycle	1st Cycle	2nd Cycle	3rd Cycle
Gas injected/ cycle, MMscf	90.0	90.0	89.8	89.8	89.8	90.0	90.0	90.0	90.0	90.0	90.0
Oil produced/ cycle, MSTB	132.4	110.0	135.9	115.6	91.1	134.4	118.2	92.7	137.0	112.5	96.2
Water produced/ cycle, MSTB	259.2	236.0	275.0	232.4	171.6	244.3	232.7	173.8	251.7	221.3	177.5
Cycle length, days	1136	1025	1109	952	789	1023	953	743	1043	905	754
Average oil rate, STB/D	117	108	122	121	116	131	124	125	131	124	128
Average water rate, STB/D	228	230	248	244	217	239	244	234	241	244	235
Oil production, Mscf injection, STB/Mscf	1.47	1.23	1.51	1.32	1.01	1.49	1.31	1.03	1.52	1.25	1.07
Cumulative oil production/cycle, % of original oil in place	7.0	5.9	7.2	6.1	4.8	7.1	6.2	5.0	7.2	6.0	5.1

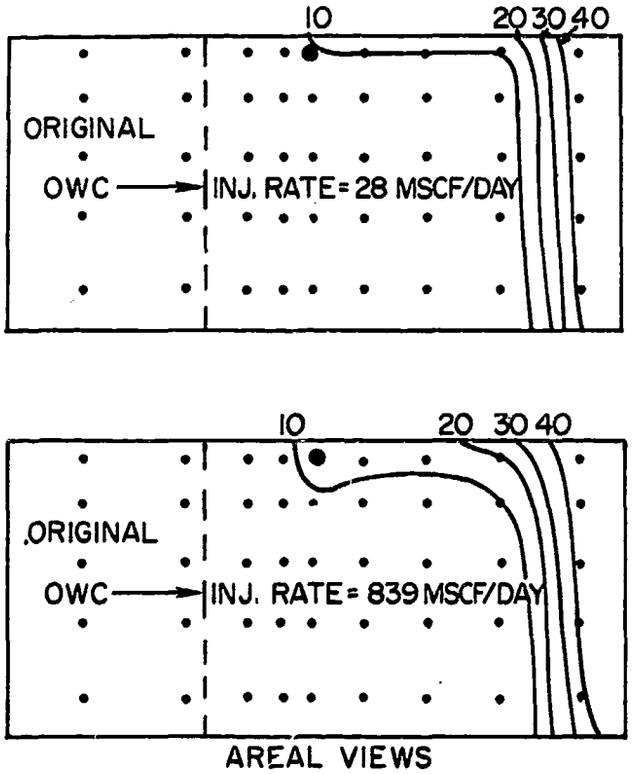

Fig. 11—Gas saturation contours at 400 MMscf gas injected.

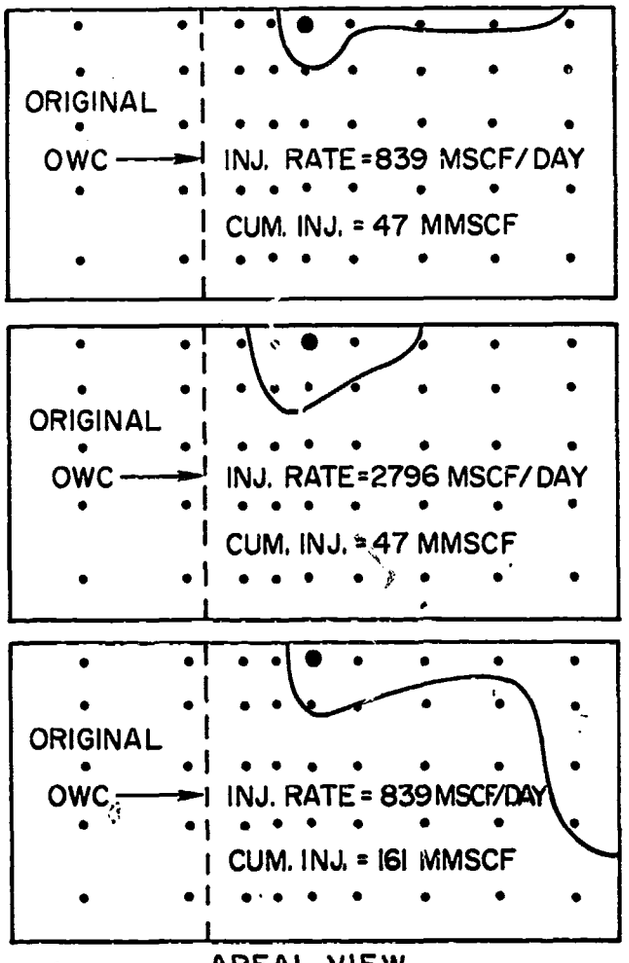

Fig. 12—5% gas saturation contour at 47 MMscf gas injected.

injection volume.

For comparison, Fig. 12 shows an areal view of a 5% gas saturation contour after 47 MMscf had been injected at rates of 839 and 2,796 Mscf/D, respectively. The saturation contours also are shown after 161 MMscf gas was injected at a rate of 839 Mscf/D. In the first view, gas was migrating uniformly to the top of the structure, while in the second view (high injection rate), the gas was moving almost radially away from the well. With continued injection at the high rate, the gas migrated both up- and downstructure, pushing oil into the water zone. In the previous section, where there was some free gas throughout the reservoir at the end of the production period, upward gas migration was independent of rate.

In the third view, all injected gas (161 MMscf) had migrated uniformly to the top of the structure, displacing oil downward. However, it was at this point of injection that oil first began moving into the water zone. This cumulative injected volume corresponds favorably with the calculated volume required to displace all the movable water.

Summary and Conclusions

Most attic oil recovery projects are performed in single-well fields, where reservoir description and data are lacking. The location of the boundaries of the reservoir and the original oil/water contact seldom are known. For this reason, it is difficult to apply conventional analytical solutions to the attic oil recovery problem. Our proposed method for calculating the required gas injection volume from the cumulative oil production provides a simple and effective means of analysis. We have shown that for reservoirs where a secondary gas cap was formed during the production cycle, the upstructure migration of gas was independent of injection rate. However, for reservoirs producing at pressures above the bubble point, the migration of gas depended on the gas injection rate. In either case, the injected gas volume was an important controllable variable in an attic oil recovery project. The maximum gas injection volume, to prevent oil from moving below the level of the original oil/water contact, could be calculated from the cumulative production and the fractional flow curves, if all produced oil was displaced with water. If a secondary gas cap formed during the production cycle and displaced oil downward, the maximum gas injection volume calculated from the cumulative production would be too high. If the reservoir had been produced at a pressure above the original bubble point, the maximum gas injection volume calculation would be too low. This occurred because a portion of the injected gas would go into solution in the undersaturated oil.

The performance of the attic oil recovery process will depend on each reservoir's unique set of rocks and fluid properties. However, based on the simulation results presented here, we can make the following general observations.

1. The most important controllable variable in a single-well project is the injected gas volume. If all produced oil has been displaced with water, this volume can be calculated from the cumulative production and the fractional flow curves.

2. For reservoirs where free gas exists at the end of the production cycle, the upstructure migration of gas is independent of injection rate. However, this does not hold for reservoirs being produced at pressures above the original bubble point.

Nomenclature

A = cross-sectional area, ft^2 (m^2)
g = gravitational constant
K_L = effective permeability to a liquid at 100% saturation, darcies
α = angle of dip of the system, degrees
μ_L = viscosity of the oil for a gas/oil system, cp (Pa·s)
$\Delta\rho$ = density difference between gas and oil for gas/oil system, g/cm^3

References

1. Morrow, R. M.: "Updip Oil Recovery by Downdip Gas Injection," *Pet. Eng.* (April 1, 1957) **29**, No. 4, 28-32.
2. Broom, J. C. and Dawsey, A. L. Jr.: "Gas Injection for Attic Oil Recovery," *Pet. Eng.* (Feb. 1959) **31**, 19-22.
3. Franklin, L. O., Koederitz, W. A. and Walker, Donald: "Recovering Attic Oil," *Oil and Gas J.* (July 24, 1961) **59**, 65-70.
4. Bleakley, W. B.: "Chevron's Attic-Oil Recovery in South Louisiana Looks Good," *Oil and Gas J.* (Nov. 13, 1967) **65**, 132-134.
5. Van Der Poel, C. and Killian, J. W.: "Attic Oil," paper 919-G presented at SPE 32nd Annual Fall Meeting, Dallas, Oct. 6-9, 1957.
6. Combs, George D. and Knezek, R. B.: "Gas Injection for Upstructure Drainage," *J. Pet. Tech.* (March 1971) 361-372.
7. Stone, H. L.: "Estimation of Three-Phase Relative Permeability and Residual Oil Data," paper presented at the CIM 24th Annual Technical Meeting, Edmonton, Canada, May 8-12, 1973.
8. Killough, J. E.: "Reservoir Simulation With History-Dependent Saturation Function," paper SPE 5106 presented at SPE 49th Annual Fall Meeting, Houston, October 6-9, 1974.
9. Thomas, L. K., Lumpkin, W. L., and Reheis, G. M.: "Reservoir Simulation of Variable Bubble Point Problems," paper SPE 5107 presented at SPE 49th Annual Fall Meeting, Houston, Oct. 6-9, 1974.
10. Jacks, H. H., Smith, O. J. E., and Mattax, C. C.: "Modeling of Three-Dimensional Reservoirs with Two-Dimensional Reservoir Simulations — The Use of Dynamic Pseudo Functions," paper SPE 4071 presented at SPE 47th Annual Fall Meeting, San Antonio, TX, Oct. 8-11, 1972.
11. Coats, K. H., Neilson, R. L., Terhune, M. H., and Weber, A. G.: "Simulation of Three-Dimensional, Two-Phase Flow in Oil and Gas Reservoirs," *Soc. Pet. Eng. J.* (Dec. 1967) 377-388.
12. Coats, K. H., Dempsey, J. R., and Henderson, J. H.: "The Use of Vertical Equilibrium in Two-Dimensional Simulation of Three-Dimensional Reservoir Performance," *Soc. Pet. Eng. J.* (March 1971) 63-71.
13. Hearn, C. L.: "Simulation of Stratified Waterflooding by Pseudo Relative Permeability Curves," *J. Pet. Tech.* (July 1971) 805-813.
14. Strickland, R. F. and Morse, R. A.: "Numerical Simulation of Gas Injection for Upstructure Drainage," PhD dissertation, Texas A&M U., College Station (Dec. 1976).
15. Terwilliger, P. L., Wiley, L. E., Hall, H. N., Bridges, P. M., and Morse, R. A.: "An Experimental and Theoretical Investigation of Gravity Drainage Performance," *Trans.*, AIME (1951) **192**, 285.

SI Metric Conversion Factors

B/D	× 1.589 873	E−01	=	m^3/d
bbl	× 1.589 873	E−01	=	m^3
ft	× 3.048*	E−01	=	m
lbm/cu ft	× 1.601 846	E−02	=	g/cm^3
MMscf/D	× 2.863 640	E−02	=	std 10^6 m^3
psia, psi	× 6.894 757	E−03	=	MPa
psi/ft	× 2.262 059	E+01	=	kPa/m
RB/MMscf	× 1.330 10	E−01	=	dm^3/kmol
sq ft	× 9.290 304	E−02	=	m^2

*Conversion factor is exact.

JPT

Original manuscript received in Society of Petroleum Engineers office Feb. 16, 1978. Paper accepted for publication Dec. 14, 1978. Revised manuscript received Aug. 22, 1979. Paper (SPE 7114) first presented at the SPE-AIME Southwest Texas Regional Meeting, held in Corpus Christi, April 14, 1978.